Emergence of long-range phase coherence in nonlocal fluids of light

A. Fusaro,[1] J. Garnier,[2] G. Xu,[1,3] C. Conti,[4,5] D. Faccio,[6] S. Trillo,[7] and A. Picozzi[1]

[1]*Laboratoire Interdisciplinaire Carnot de Bourgogne (ICB), UMR 6303 CNRS–Université Bourgogne Franche-Comté, F-21078 Dijon, France*

[2]*Centre de Mathématiques Appliquées, Ecole Polytechnique, 91128 Palaiseau Cedex, France*

[3]*Univ. Lille, CNRS, UMR 8523, PhLAM–Physique des Lasers Atomes et Molécules, F-59000 Lille, France*

[4]*Dipartimento di Fisica, Università di Roma La Sapienza, 00185 Rome, Italy*

[5]*Institute for Complex Systems, National Research Council (ISC-CNR), Via dei Taurini 19, 00185 Rome, Italy*

[6]*School of Engineering and Physical Sciences, SUPA, Heriot-Watt University, Edinburgh EH14 4AS, United Kingdom*

[7]*Department of Engineering, University of Ferrara, Via Saragat 1, 44122 Ferrara, Italy*

(Received 20 March 2017; revised manuscript received 9 May 2017; published 14 June 2017)

The emergence of long-range phase coherence among random nonlinear waves is a fascinating effect that characterizes fundamental phenomena such as the condensation of nonlinear waves and the related manifestation of superfluidity of certain turbulent flows. Here we report a previously unrecognized phenomenon of spontaneous emergence of long-range phase coherence among incoherent waves interacting through a nonlocal nonlinearity. The theory reveals that the establishment of long-range phase coherence constitutes a generic property of a conservative (Hamiltonian) system of highly nonlocal random waves that evolve in the strongly nonlinear regime. Aside from phase coherence, the field exhibits intensity fluctuations whose coherence length is shown to increase in a dramatic way during the evolution of the system. The analysis can be transposed to the temporal domain, revealing the emergence of temporal phase coherence among incoherent waves propagating in nonlinear materials featured by a noninstantaneous nonlinear response.

DOI: 10.1103/PhysRevA.95.063818

I. INTRODUCTION

Understanding the mechanisms responsible for self-organization processes in conservative and reversible Hamiltonian wave systems is an arduous problem that generated significant interest. Contrary to dissipative systems, a conservative Hamiltonian system cannot evolve towards a fully ordered state, because such an evolution would imply a loss of statistical information for the system that would violate its formal reversibility. However, despite formal reversibility, a nonintegrable Hamiltonian wave system is expected to exhibit an irreversible evolution toward an equilibrium state, as a result of an irreversible process of diffusion in phase space [1]. In this regard, an important achievement was accomplished when Zakharov and collaborators reported in Ref. [2] numerical simulations of the focusing nonintegrable nonlinear Schrödinger equation (NLSE). This study revealed that the Hamiltonian system evolves, as a general rule, towards an ordered state characterized by a "big soliton" in the midst of small-scale turbulent fluctuations. In this "soliton turbulence" scenario, the solitary wave plays the role of a "statistical attractor" for the Hamiltonian system, while the small-scale fluctuations store the information necessary for time reversal [3–7].

The phenomenon of condensation of classical waves in the defocusing regime of the NLSE is another important example of self-organization process that occurs in Hamiltonian wave systems [7–13], which can be viewed as a classical analog of the quantum Bose-Einstein condensation process [14–20]. From a broader perspective, condensation-like phenomena have been the subject of a great interest in optical systems [21–27]. It is important to note that, at variance with the "soliton turbulence" scenario, the process of wave condensation is known to be characterized by the emergence of long-range order and phase coherence, in the sense that the correlation function of the wave amplitude does not decay to zero at infinity [17]. This property of long-range phase coherence is fundamental, for instance, for the manifestation of superfluidity or the generation of Bogoliubov sound waves in optical wave systems [17,28]. This area of research has been mainly developed in dissipative cavity systems in the past [28–32], and it is now attracting a growing interest in conservative free propagation in nonlinear optical bulk materials [33–37].

Our aim in this article is to report a phenomenon of spontaneous emergence of long-range phase coherence in a system of conservative random waves. The nonlinear mechanism underlying the formation of phase coherence relies on the property of nonlocality. A nonlocal wave interaction means that the response of the nonlinearity at a particular point is not determined solely by the intensity at that point, but also depends on the wave intensity in its vicinity. Nonlocality thus constitutes a generic property of a large number of nonlinear wave systems [6,38–64]. A wave turbulence approach of the problem revealed that the evolution of random waves in the highly nonlocal regime can be described in detail by a long-range Vlasov formalism [21,67–69]. This unveiled an interesting analogy between nonlocal turbulent flows and collective dynamical behaviors inherent to systems of particles with long-range interactions, such as gravitational systems (e.g., formation of galaxies) or two-dimensional (2D) geophysical fluid flows (e.g., Jupiter red spot) [70]. However, this Vlasov-like kinetic approach did not reveal the underlying critical coherent phase effects that characterize nonlocal incoherent waves.

In this article, we show that the emergence of long-range phase coherence constitutes a robust and generic property of a highly nonlocal random wave system that evolves in the strongly nonlinear regime. In particular, long-range phase coherence is shown to emerge irrespective of the

dimensionality of the system or the sign of the nonlinearity, which can be either focusing or defocusing. In addition, the analysis of the coherence properties of intensity fluctuations reveals that the coherence length can increase in a dramatic way during the propagation of the waves. This work then reports a previously unrecognized fundamental mechanism of spontaneous formation of long-range phase coherence in a conservative (Hamiltonian) system of random waves, a feature which is at the root of several fascinating phenomena in the emergent key area of the quantum fluids of light, such as the supersonic to superfluid transition and the associated nucleation of quantized vortices in the wake of an obstacle [28,33,37].

II. NUMERICAL SIMULATIONS

A. NLSE model

The nonlocal nonlinear Schrödinger equation (NLSE) is known as a universal model describing the evolution of waves in the presence of nonlocal nonlinearities. In the context of optics, the NLSE models the transverse spatial evolution of an optical beam that propagates in a material featured by a nonlocal nonlinear response [48–57,59], e.g., thermal media [36,37,41–47], or nematic liquid crystals [6,38–40]. From a broader perspective, nonlocal nonlinearities are found in several physical systems, such as dipolar Bose-Einstein condensates [60], roton excitations in superfluids [61], atomic vapors [62,63], or plasmas [64]. The evolution of the field can be modeled by the following generic form of the NLSE equation:

$$i\,\partial_z\psi = -\frac{\alpha}{2}\nabla^2\psi + \gamma\,\psi \int U(|\boldsymbol{r}-\boldsymbol{r}'|)|\psi|^2(\boldsymbol{r}',z)\,d\boldsymbol{r}', \quad (1)$$

where the dynamics occurs in the two-dimensional transverse plane $\boldsymbol{r}=(x,y)$ and the propagation length z plays the role of time. The diffraction parameter is $\alpha = 1/\beta_0$, where β_0 denotes the wave vector of the laser beam, while σ is the spatial extension of the nonlocal response function $U(\boldsymbol{r})$, i.e., the range of nonlocal interaction. In the following we will focus the presentation into the defocusing regime $\gamma > 0$, while the focusing case ($\gamma < 0$) will be discussed later. In addition to the total "power" of the field, $\mathcal{N} = \int |\psi|^2(\boldsymbol{r},z)d\boldsymbol{r}$, we note that the NLSE (1) conserves the Hamiltonian, $\mathcal{H} = \mathcal{E} + \mathcal{U}$, which has a linear contribution $\mathcal{E}(z) = \frac{\alpha}{2}\int |\nabla\psi|^2(\boldsymbol{r},z)\,d\boldsymbol{r}$, and a nonlinear contribution, $\mathcal{U}(z) = \frac{\gamma}{2}\iint |\psi|^2(\boldsymbol{r},z)\,U(|\boldsymbol{r}-\boldsymbol{r}'|)\,|\psi|^2(\boldsymbol{r}',z)\,d\boldsymbol{r}\,d\boldsymbol{r}'$. It proves convenient to introduce an effective nonlinear length $L_0 = 1/(\gamma I_0)$, where the intensity reads $I_0 = \mathcal{N}/L^2$, L being the spatial size of the numerical window. In this way, the "healing length" $\Lambda = \sqrt{\alpha L_0}$ provides the characteristic spatial scale for which linear and nonlinear effects are of the same order of magnitude ($\mathcal{E} \sim \mathcal{U}$). Note in this respect that $\Lambda = \lambda_c$ is equivalent to $L_0 = L_d$, where $L_d = \lambda_c^2/\alpha$ is the characteristic propagation length associated to linear diffraction effects, λ_c being the transverse correlation length of the wave. We anticipate that phase coherence will be shown to emerge in the strongly nonlinear regime $L_0 \ll L_d$ (or $\lambda_c \gg \Lambda$).

In the numerical simulations we use periodic boundary conditions in $\boldsymbol{r}$ space, with a numerical spatial window much larger than the nonlocal range $L \gg \sigma$. To avoid numerical artifacts, we consider the illustrative example of a rapidly decaying Gaussian-shaped response function $U(r) = (2\pi\sigma^2)^{-1}\exp[-r^2/(2\sigma^2)]$, with $r = |\boldsymbol{r}|$. However, we stress the important fact that the phenomenon of spontaneous emergence of long-range phase coherence is general and does not depend on the specific form of the response function; we will see that it even takes place in the temporal domain for a response function that is constrained by the causality condition (see Sec. V B). Also notice that, although we focus the presentation of the emergence of phase coherence in two spatial dimensions, this effect can also occur in one dimension (or in three dimensions), as will be discussed later.

In the simulations, the initial random wave $\psi_0(\boldsymbol{r})$ refers to an incoherent speckle beam whose envelope profile is localized in space $|\psi_0|^2(\boldsymbol{r}) \sim \exp(-r^2/\Delta^2)$. The incoherent beam is characterized by a Gaussian spectrum $|\tilde{\psi}_0|^2(\boldsymbol{k}) \sim \exp(-k^2/\delta_k^2)$ with random spectral phases, so that the initial correlation length is $\lambda_c \simeq 2\pi/\delta_k$, and the typical size of the speckles is much smaller than both the beam size ($\lambda_c \ll \Delta$) and the nonlocal range ($\lambda_c \ll \sigma$). We consider a small numerical grid size so as to properly resolve all the fluctuations of the incoherent wave during its propagation. For each individual realization of the initial random function $\psi_0(\boldsymbol{r})$, the coherence properties of the wave evolve during the propagation in a deterministic fashion, as described by the solution $\psi(\boldsymbol{r},z)$ of the deterministic NLSE (1).

Before discussing the numerical results, let us briefly comment on the particular example of a thermal nonlinearity [36,37,41–46]. A thermal nonlinearity originates in the diffusion of heat in the nonlinear medium, which is in principle an isotropic process, so that the corresponding nonlinear response should also be isotropic, i.e., the function U should depend on the longitudinal variable z. We note in this respect that the smallest longitudinal z-scale variation of the field $\psi(\boldsymbol{r},z)$ is given by the nonlinear length L_0, since we deal with the strongly nonlinear regime $L_0 \ll L_d$ (or equivalently $\lambda_c \gg \Lambda$). Assuming that $\lambda_c \ll \sigma \ll L_0$, the three-dimensional convolution involved in the nonlinear term of the generalized NLSE is important in the transverse direction, since the intensity $|\psi|^2(\boldsymbol{r},z)$ exhibits small fluctuations in $\boldsymbol{r}$ at the scale σ ($\lambda_c \ll \sigma$). However, the convolution is not important in the longitudinal direction, since the field $\psi(\boldsymbol{r},z)$ does not vary in z at the scale $\sigma \ll L_0$. Accordingly, the convolution in the longitudinal z direction can be neglected, so that one recovers the effective two-dimensional convolution in the NLSE given in Eq. (1). We also note that the effective nonlocal range σ strongly depends on the boundary conditions imposed by the nonlinear sample to solve the three-dimensional heat equation. In this way, despite the fact that the nonlinear response function is in principle "infinite range" [44,45], the boundary conditions introduce an effective finite range for the response function [65]. It is important to note that the effective 2D response function in the NLSE has been widely considered to study nonlocal dynamical effects [41,50–52,55–57], and that this model proved successful to capture details of various experiments realized in thermal nonlinear media, see, e.g., Refs. [36,37,42,43,47,68].

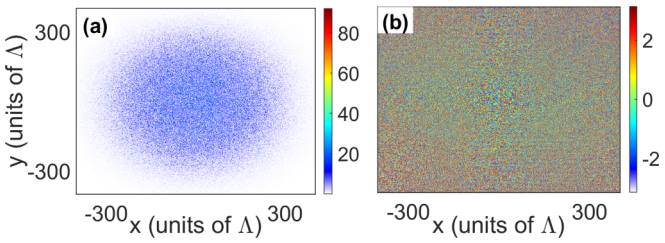

FIG. 1. Numerical simulation of the NLSE starting from an initial random wave with linear and nonlinear effects of the same order ($\mathcal{U}_0 \simeq \mathcal{E}_0$, or $\lambda_c \simeq \Lambda$). Spatial distribution of the intensity $|\psi|^2(\boldsymbol{r})$ (a), and corresponding (modulo 2π) phase $\phi(\boldsymbol{r})$ (b), at $z = 30L_0$: No long-range phase coherence emerges in the system. Parameters are $\mathcal{U}_0/\mathcal{E}_0 \simeq 0.85$, $L = 1200\Lambda$, $\sigma = 100\Lambda$, width of the initial incoherent beam $\Delta \simeq 120\Lambda$.

B. Emergence of phase coherence

We have performed numerical simulations of the NLSE (1) in order to get physical insight into the emergence of phase coherence. We compare the propagation regime where linear and nonlinear effects are of the same order at $z = 0$, i.e., $\lambda_c \sim \Lambda$ ($\mathcal{U}_0 \sim \mathcal{E}_0$), with the strongly nonlinear propagation regime, $\lambda_c \gg \Lambda$ ($\mathcal{U}_0 \gg \mathcal{E}_0$). The simulations reported in Figs. 1 and 2 reveal that, in marked contrast to the weakly nonlinear regime where the system exhibits a random phase dynamics (Fig. 1), the strongly nonlinear interaction is responsible for the spontaneous emergence of a well-structured spatial phase distribution, as remarkably illustrated in Fig. 2. Phase coherence is characterized by almost

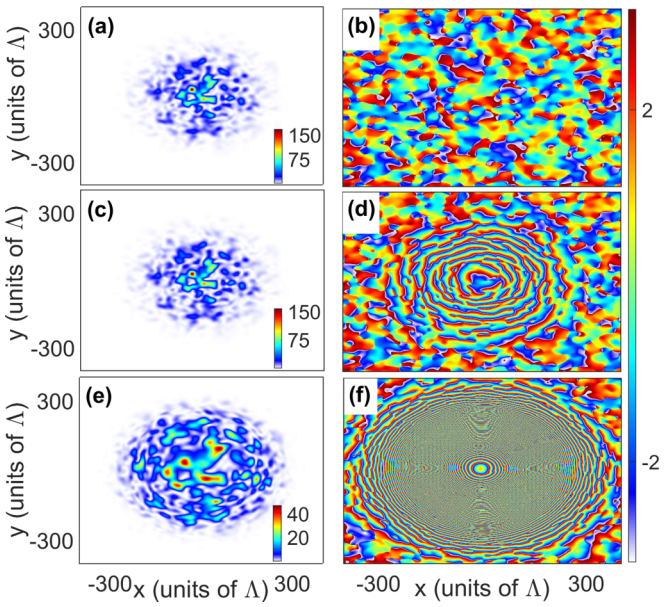

FIG. 2. Numerical simulation of the NLSE starting from an initial random wave in the strongly nonlinear regime, $\mathcal{U}_0/\mathcal{E}_0 \gg 1$ (or $\lambda_c \gg \Lambda$). Spatial distribution of the intensity $|\psi|^2(\boldsymbol{r})$ (first column) and the (modulo 2π) phase $\phi(\boldsymbol{r})$ (second column) at $z = 0$ (a–b), $z = 4L_0$ (c–d), $z = 30L_0$ (e–f). At variance with Fig. 1, in the strongly nonlinear regime long-range phase coherence emerges in the system. Parameters are $\mathcal{U}_0/\mathcal{E}_0 \simeq 480$ (or $\lambda_c \simeq 66\Lambda$), $L = 1200\Lambda$, $\sigma = 100\Lambda$, width of the initial incoherent beam $\Delta \simeq 120\Lambda$.

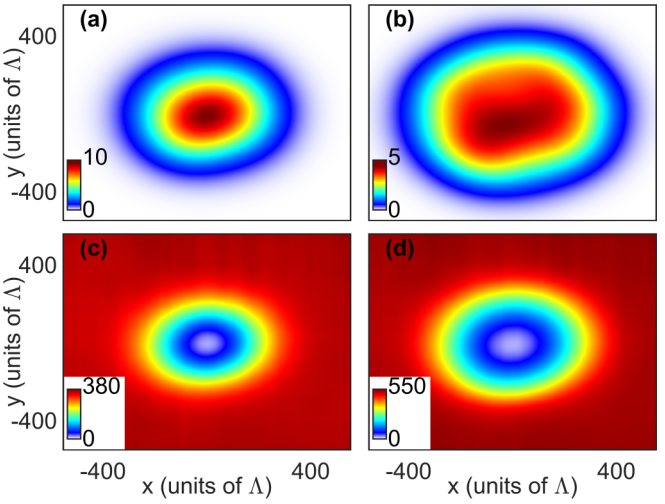

FIG. 3. Numerical simulation of the NLSE showing the effective potential $V(\boldsymbol{r})$ (first line), and unwrapped spatial phase $\phi(\boldsymbol{r})$ of the random field $\psi(\boldsymbol{r},z)$ (second line), at $z = 30L_0$ for (a) and (c) and $z = 55L_0$ for (b) and (d). These plots correspond to the simulation reported in Fig. 2 in the strongly nonlinear regime ($\mathcal{U}_0 \gg \mathcal{E}_0$): The emergence of phase coherence is mediated by the long-range effective potential, $V(\boldsymbol{r})$.

radially symmetric spatial oscillations of the phase profile, whose typical period decreases with the radial coordinate (distance from the beam center, r), as well as the propagation length (z). It is important to note in Fig. 2 that phase coherence is established over the whole surface of the beam; the analysis will reveal that phase coherence emerges over the large length scale $\sigma \gg \lambda_c$. In contrast to such a long-range phase coherence, the speckle beam exhibits pronounced intensity fluctuations (left column in Fig. 2), which are characterized by an expansion of the correlation length during the propagation, a feature that will be described in detail by the theory [see Eq. (19)]. In this way, the intensity of the beam resembles a "speckle beam." However, at variance with a conventional speckle, here the fluctuations of the beam are phase-correlated to each other by the underlying long-range phase coherence. We underline the important fact that the formation of phase coherence is clearly apparent for each individual realization of the initial random wave $\psi_0(\boldsymbol{r})$, i.e., for each simulation of the NLSE; the emergence of phase coherence does not require an averaging over the realizations of the random function $\psi_0(\boldsymbol{r})$.

We finally note that very similar results as those reported in Figs. 1–3 have been obtained with a thermal response function of the form $U(r) = K_0(r/\sigma)/(2\pi\sigma)$, where $K_0(x)$ is the modified Bessel function of second kind (see, for instance, Ref. [68]).

III. HYDRODYNAMIC FORMULATION

A. Fluid-like description

To explain the numerical observations, we follow the usual procedure based on the Madelung transformation and

decompose the wave amplitude as $\psi(\boldsymbol{r},z)=\sqrt{\rho(\boldsymbol{r},z)}\exp(i\phi(\boldsymbol{r},z))$, so that the NLSE (1) takes the form

$$\partial_z\rho+\alpha\boldsymbol{\nabla}\cdot(\rho\boldsymbol{\nabla}\phi)=0, \tag{2}$$

$$\partial_z\phi+\frac{\alpha}{2}(\nabla\phi)^2+V=\frac{\alpha}{2\sqrt{\rho}}\nabla^2\sqrt{\rho}, \tag{3}$$

where we have introduced the effective potential

$$V(\boldsymbol{r},z)=\gamma\int U(|\boldsymbol{r}-\boldsymbol{r}'|)|\psi|^2(\boldsymbol{r}',z)\,d\boldsymbol{r}'. \tag{4}$$

The last term in (3) refers to the analog of the Bohm quantum potential [66]. In the strongly nonlinear regime considered here $\lambda_c\gg\Lambda$, the potential $V(\boldsymbol{r})$ in (3) dominates the linear diffraction effects described by the quantum potential and the term $(\nabla\phi)^2$. On the other hand, the intensity $\rho(\boldsymbol{r})$ is simply advected by the transport equation (2), and its feedback to the phase dynamics remains negligible compared to V and $(\nabla\phi)^2$ in the regime $\lambda_c\gg\Lambda$. The fact that the quantum potential term can be neglected with respect to the term $(\nabla\phi)^2$ is clearly apparent in the numerical simulations shown in Fig. 2: At variance with the speckle fluctuations of the intensity $\rho(\boldsymbol{r})$ that exhibit a slow expansion during the propagation, the phase $\phi(\boldsymbol{r})$ undergoes very rapid radial oscillations. We will see theoretical arguments in Sec. IV D to justify that the quantum potential term can be indeed neglected. Then introducing the analog of the momentum, $\boldsymbol{u}=\boldsymbol{\nabla}\phi$, Eqs. (2) and (3) reduce to

$$\partial_z\rho+\alpha\boldsymbol{\nabla}\cdot(\rho\,\boldsymbol{u})=0, \tag{5}$$

$$\partial_z\boldsymbol{u}+\alpha(\boldsymbol{u}\cdot\boldsymbol{\nabla})\boldsymbol{u}+\boldsymbol{\nabla}V=0. \tag{6}$$

Note that it is also possible to derive Eqs. (5) and (6) in a formal way from Eqs. (2) and (3) in the strongly nonlinear regime ($\lambda_c\gg\Lambda$) by following the well-known WKB expansion procedure; see Ref. [41] for the application of the method to the specific example of the nonlocal NLSE considered here.

The type of hydrodynamic Eqs. (5) and (6) are hyperbolic and are known to exhibit finite "time" shock singularities in the defocusing regime considered here [71]. This aspect has been widely studied in different configurations [72–79], in particular in the presence of nonlocal nonlinearities [41–43,80,81]. It is worth pointing out that, in thermal media, the oscillatory ring structure of the dispersive shock induced by the defocusing effect over Gaussian laser beams have been reported much earlier (though not explicitly labeled as a shock) by independent groups [82–84], and interpreted in terms of ray crossing and spherical aberration of the self-induced thermal lens [85]. We also note that shock singularities have been considered in the presence of a structural disorder of the nonlinear medium [86,87], while perfectly deterministic (coherent) wave amplitudes have been assumed. At variance with these previous works, here we deal with the evolution of an *initial incoherent wave* [68,88]; the intensity and momentum in Eqs. (5) and (6) refer to random functions at any z. In this framework, collective incoherent shock singularities have been reported in Refs. [68,69] on the basis of singular solutions of the long-range Vlasov equation. However, as already commented, this kinetic approach is not appropriate to study the emergence of phase coherence among the random waves, whose study constitutes the main purpose of the present article.

B. Criterion for the emergence of phase coherence

The starting point of our analysis is the simple observation that, as a result of the convolution involved in the nonlinear term of the NLSE, the response function $U(r)$ averages out the fluctuations of the intensity of the random wave $\rho(\boldsymbol{r})$ in the long-range interaction regime ($\sigma\gg\lambda_c$). This means that the effective potential (4) can be approximated by $V(\boldsymbol{r},z)\simeq\gamma\int U(|\boldsymbol{r}-\boldsymbol{r}'|)\langle\rho(\boldsymbol{r}',z)\rangle d\boldsymbol{r}'$, where $\langle\cdot\rangle$ denotes an average over the realizations of the initial random field, $\psi(\boldsymbol{r},0)$. This merely explains why the potential $V(\boldsymbol{r})$ turns out to be a smooth function over the large scale σ. This property is clearly visible in the simulations, as remarkably revealed by the comparison of the intensity fluctuations of $\rho(\boldsymbol{r})$ in Fig. 2 and the smoothed profile of the effective potential $V(\boldsymbol{r})$ reported in Figs. 3(a)–3(b). On the other hand, the momentum $\boldsymbol{u}(\boldsymbol{r},z)$ involved in the second Burgers term of Eq. (6) is a random function that rapidly fluctuates on the small spatial scale λ_c. Accordingly, the driving force $\boldsymbol{\nabla}V(\boldsymbol{r})$ is expected to lead to the formation of phase coherence over a large surface section (of the order $\sim\sigma^2$) whenever this force dominates the second Burgers term in (6).

In order to qualitatively assess the relative contributions of the two terms involved in Eq. (6), it proves convenient to rescale the functions by introducing the parameter $\varepsilon=1/\sigma$: $U(\boldsymbol{r})=\varepsilon^2U_0(\boldsymbol{R})$ and $\rho(\boldsymbol{r},z)=L^2\varepsilon^2I_0\rho_0(\boldsymbol{R},Z)$, with $\boldsymbol{R}=\varepsilon\boldsymbol{r}$ and $Z=\varepsilon z$. The typical widths of $\rho_0(\boldsymbol{R},Z)$ and $U_0(\boldsymbol{R})$ are now of order one with $\int\rho_0(\boldsymbol{R})\,d\boldsymbol{R}=1$ and $\int U_0(\boldsymbol{R})\,d\boldsymbol{R}=1$, which thus gives $\boldsymbol{\nabla}V\sim\gamma\mathcal{N}/\sigma^3$. On the other hand, the Burgers term in (6) is of order $\alpha(\boldsymbol{u}\cdot\boldsymbol{\nabla})\boldsymbol{u}\sim\alpha/\lambda_c^3$. This reveals that, whenever $\lambda_c^3\gamma\mathcal{N}/(\alpha\sigma^3)\gg1$, the force $\boldsymbol{\nabla}V$ dominates the behavior of $\boldsymbol{u}$ in Eq. (6). Furthermore, considering that $\rho\sim\mathcal{N}/\sigma^2$, we see that long-range phase coherence emerges in the system provided that the criterion $\lambda_c^3\gamma\rho/(\alpha\sigma)\gg1$ is satisfied. It proves convenient to rewrite the criterion in term of the healing length, which is

$$\frac{(\rho/I_0)(\lambda_c/\Lambda)^3}{\sigma/\Lambda}\gg1. \tag{7}$$

Considering that $\rho/I_0\gtrsim1$ (since $L>\sigma$) and recalling that $\lambda_c\gg\Lambda$ in the strongly nonlinear regime, then the criterion (7) turns out to be almost systematically satisfied. As a matter of fact, it is quite difficult and rather artificial to find a regime in which the criterion is not verified, since it would require a typical value of nonlocal nonlinearity at least three orders of magnitude larger than the healing length, $\sigma/\Lambda\gg10^3$.

It is important to stress that this analysis is general. In particular, it holds *a priori* for any form of the response function $U(r)$, provided it exhibits the highly nonlocal property ($\sigma\gg\Lambda$). The analysis also holds irrespective of the sign of the nonlinearity, which can be either defocusing or focusing. In addition, the criterion (7) is valid for any spatial dimension of the system (a feature that will be discussed later in the temporal and spatio-temporal domains). This reveals that the emergence of long-range phase coherence constitutes a generic property of highly nonlocal wave systems that evolve in the strongly nonlinear regime.

IV. COHERENCE PROPERTIES

A. Correlations along the characteristics

We pursue our study through the analysis of the coherence properties of the random wave. The subsequent analysis is apparently similar to that reported in Ref. [68] in the framework of the Vlasov formalism. However, *at variance with such a statistical approach, which is inherently based on an average over the realizations*, here we analyze the fluctuations of the incoherent field $\psi(\boldsymbol{r},z)$ for an individual realization of the initial random functions $(\rho_0(\boldsymbol{r}),\boldsymbol{u}_0(\boldsymbol{r}))$. In other terms, the subsequent analysis does not rely on an averaging over the realizations of the initial conditions.

We first note that, because of the long-range interaction $\sigma \gg \lambda_c$, the effective potential $V(\boldsymbol{r},z)$ is an almost radially symmetric function. According to the criterion (7), the driving term $\boldsymbol{\nabla} V(r) = V'(r)\boldsymbol{r}/r$ dominates the evolution of the momentum in (6), so that the momentum turns radially outgoing, i.e., $\boldsymbol{u} = u(r,z)\boldsymbol{r}/r$ for z large enough to neglect the initial noisy condition, $\boldsymbol{u}_0(\boldsymbol{r})$. The hydrodynamic Eqs. (5) and (6) can thus be reduced to the following system:

$$\partial_z \check{\rho} + \alpha \partial_r(\check{\rho} u) = 0, \tag{8}$$

$$\partial_z u + \alpha u \partial_r u + \partial_r V = 0, \tag{9}$$

where $\check{\rho}(r,\theta,z) = r\rho(r,\theta,z)$, and the effective nonlinear potential is given by $V(r,z) = \gamma \int \tilde{U}(r,r')\langle\rho(r',\theta,z)\rangle r'\,dr'$, with $\tilde{U}(r,r') = \int_0^{2\pi} U(\sqrt{r^2+r'^2-2rr'\cos\theta})\,d\theta$. Note that the mean $\langle\rho(r,\theta,z)\rangle$ is independent of the polar angle θ, because it is independent of θ at $z=0$ (the initial mean intensity is radially symmetric) and the system preserves this property during the propagation.

Despite the random character of the functions $(\check{\rho}(\boldsymbol{r},z),u(r,z))$, the system (8) and (9) can be solved by making use of the method of the characteristics. We define the following quantities $w(z) = u(R(z),z)$, $\tau(z) = \partial_z u(R(z),z)$, $\xi(z) = \partial_r u(R(z),z)$, $\check{\varrho}(z) = \check{\rho}(R(z),\theta,z)$ for a fixed and arbitrary value of the polar angle θ. These functions can be shown to satisfy the following system of ordinary differential equations:

$$\frac{dR}{dz} = \alpha w(z), \quad R(0) = r_0, \tag{10}$$

$$\frac{dw}{dz} = \tau(z) + \alpha w(z)\xi(z), \quad w(0) = w_0, \tag{11}$$

$$\frac{d\tau}{dz} = -\partial_{zr}^2 V(R(z),z) - \alpha\xi(z)\tau(z), \quad \tau(0) = -\partial_r V_0(r_0), \tag{12}$$

$$\frac{d\xi}{dz} = -\partial_r^2 V(R(z),z) - \alpha\xi^2(z), \quad \xi(0) = \xi_0, \tag{13}$$

$$\frac{d\check{\varrho}}{dz} = -\alpha\xi(z)\check{\varrho}(z), \quad \check{\varrho}(0) = r_0\rho_0(r_0,\theta). \tag{14}$$

We recall that, following a procedure similar to that developed in Ref. [68], the gradient of the momentum and the intensity exhibit a finite "time" singularity at some propagation length, say, z_∞. In the following we study more specifically the coherence properties of the intensity fluctuations before the singularity $z < z_\infty$, in the regime where phase coherence emerges in the system, i.e., the criterion (7) is satisfied. Accordingly, the equation for the momentum reduces to $\partial_z u + \partial_r V = 0$. In order to pursue our study in analytic form, we neglect the "time" evolution of the potential $V(r)$, which is justified when the nonlocal range is much larger than the width of the initial incoherent beam, $\Delta \ll \sigma$. In this way, $u(r,z) = -\partial_r V(r)z$, and defining $\tilde{R}(r_0,s) = R(r_0,\sqrt{s})$ with $r_0 = R(r_0,z=0)$ and $s = z^2$, we obtain from (10)

$$\frac{d\tilde{R}}{ds} = -\frac{\alpha}{2}\partial_r V(\tilde{R}), \quad \tilde{R}(r_0,0) = r_0. \tag{15}$$

We also define $\tilde{\varrho}(r_0,\theta,s) = \check{\varrho}(r_0,\theta,\sqrt{s})$, so that (14) reads

$$\frac{d\tilde{\varrho}}{ds} = \frac{\alpha}{2}\partial_r^2 V(\tilde{R})\tilde{\varrho}, \quad \tilde{\varrho}(r_0,\theta,0) = \check{\rho}_0(r_0,\theta), \tag{16}$$

which can be integrated as

$$\tilde{\varrho}(r_0,\theta,s) = \check{\rho}_0(r_0,\theta)\frac{\partial_r V(r_0)}{\partial_r V(\tilde{R}(r_0,s))}.$$

Making use of the reversible property of the evolution along the characteristics [i.e., $r_0 = \tilde{R}(r,s)$ if and only if $\tilde{R}(r_0,-s) = r$], we can write the evolution of the intensity of the random field in the form

$$\check{\rho}(r,\theta,z) = \check{\rho}_0(\tilde{R}(r,-z^2),\theta)\frac{\partial_r V(\tilde{R}(r,-z^2))}{\partial_r V(r)}. \tag{17}$$

This expression shows that the initial intensity fluctuations $\rho_0(\boldsymbol{r})$, are transported along the characteristics, and they can be either compressed or expanded depending on their relative positions in the incoherent beam.

We illustrate the meaning of Eq. (17) by considering the concrete example of a potential of the form, $V(r) = V_0/(1+\nu r^2)$. The detailed evolution of the intensity fluctuations depend on the specific form of the potential, however, the qualitative description we are going to present is preserved with any smooth and decaying effective potential, as will be confirmed by the simulations. Equation (15) can then be integrated in explicit form, yielding

$$\tilde{R}(r,-z^2) = g_\nu^{-1}(g_\nu(r) - \nu\alpha V_0 z^2), \tag{18}$$

where $g_\nu(r) = \log(r) + \nu r^2 + \nu^2 r^4/4$, and g_ν^{-1} is the inverse function of g_ν.

B. Correlations in the center of the incoherent beam

Let us first consider a point in the center of the beam $\nu r^2 \ll 1$, so that Eq. (18) readily gives the characteristics, $R(z) = r_0\exp(\nu\alpha V_0 z^2)$. According to Eq. (17), the evolution of the field intensity then reads

$$\rho(r,\theta,z) = \rho_0\big(re^{-\nu\alpha V_0 z^2},\theta\big)e^{-2\nu\alpha V_0 z^2}. \tag{19}$$

This expression remarkably reveals that the correlation radius increases by the factor $\exp(\nu\alpha V_0 z^2)$, while the mean intensity is damped by $\exp(-2\nu\alpha V_0 z^2)$. We stress the fact that this dramatic increase of the coherence length is not simply related to the diffraction of the whole beam, since such a coherence enhancement occurs in the initial stage of propagation where the effective potential is assumed constant, $V(r) \simeq$ const. This unexpected increase of coherence of the beam has been

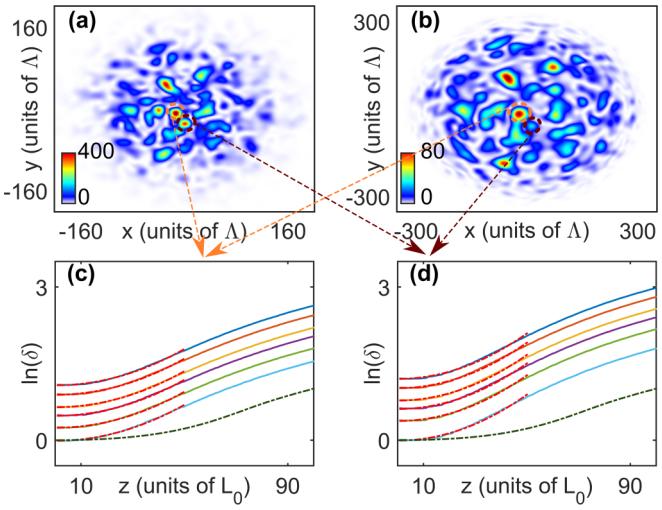

FIG. 4. Intensity fluctuations: (a–b) Evolution of the intensity pattern obtained by simulation of the NLSE (1) in the strongly nonlinear regime ($\mathcal{U}_0 \gg \mathcal{E}_0$ or $\lambda_c \gg \Lambda$): $z = 0$ (a), $z = 50L_0$ (b). (c–d) Corresponding evolutions of the sizes [$\ln(\delta)$ vs z] of two particular speckles (brown- and red-encircled), for six different values of their intensity levels: The dramatic increase of the coherence length $\sim \exp(\nu\alpha V_0 z^2)$ is in agreement with the theory [Eq. (19)]; see the parabolic dot-dashed red lines for $z \leqslant 50L_0$. The dashed dark line shows the corresponding evolution of the width of $V(r)$ – note that $V(r) \simeq$ const for $z \lesssim 40L_0$, so that the coherence enhancement of intensity fluctuations is not due to the beam expansion. Parameters are width of the initial incoherent beam $\Delta \simeq 80\Lambda$, $\mathcal{U}_0/\mathcal{E}_0 \simeq 330$, $L = 1500\Lambda$, $\sigma = 150\Lambda$.

confirmed by NLSE simulations, as remarkably illustrated in Fig. 4, where $V(r) \simeq$ const for $z \lesssim 40$. It is important to note that this good agreement has been obtained for a large variety of realizations of the initial random function $\rho_0(\boldsymbol{r})$ and for diverse choices of the speckles that have been analyzed, even those for which the correlation expansion is not apparent, as in Fig. 4(d).

C. Parabolic-shaped phase coherence

The analysis that we have developed also provides the evolution of the phase of the field in the central region of the incoherent beam, $\nu r^2 \ll 1$. As discussed above, the phase dynamics is driven by the effective potential, $u(R(z),z) = -\partial_r V(R(z))z$. Accordingly, the phase evolves according to

$$\phi(r,z) = \phi_0(r) + \nu V_0 r^2 z. \tag{20}$$

As the beam propagates, the initial random phase $\phi_0(r)$ becomes negligible with respect to the second driving term in (20), which thus shows that phase coherence emerges very rapidly (for small propagation lengths) in the central region of the beam. More precisely, Eq. (20) reveals that the oscillations of the (modulo 2π) phase increase linearly during the propagation $\sim z$, and quadratically with the radial distance from the beam center $\sim r^2$. To properly verify this theoretical prediction, we considered a highly nonlocal regime, in such a way that the effective potential remains almost constant for relatively large propagation lengths. As illustrated

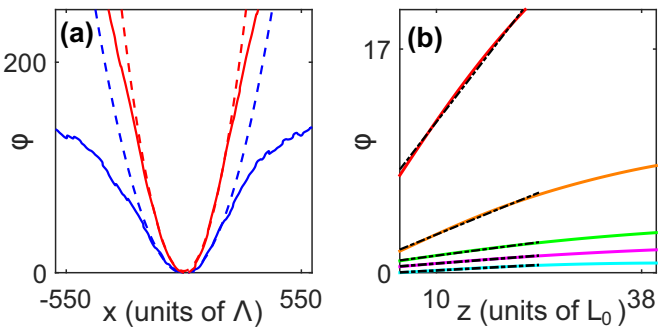

FIG. 5. Properties of phase coherence: Numerical simulations of the NLSE (1) in the strongly nonlinear regime $\mathcal{U}_0 \gg \mathcal{E}_0$ (or $\lambda_c \gg \Lambda$). (a) Unwrapped phase $\phi(x, y = 0)$ at $z = 15L_0$ (blue line), $z = 45L_0$ (red line); the spatial phase exhibits a parabolic-shaped profile (dashed blue and red lines) for large z, in agreement with the theoretical prediction of Eq. (20). (b) Evolution of the phase with respect to the propagation length z, for $r = 10$, 20, 30, 50, 100 in units of Λ (from the bottom to the top). The dashed dark line shows the linear behavior predicted by Eq. (20); note that $V(r) \simeq$ const for $z \lesssim 25L_0$. Parameters are $\mathcal{U}_0/\mathcal{E}_0 \simeq 220$, $\sigma = 200\Lambda, \Delta \simeq 80\Lambda, L = 1500\Lambda$.

in Fig. 5, the prediction (20) is well confirmed by NLSE simulations. Note, however, that, at variance with the effect of coherence enhancement discussed above through Fig. 4, here the formation of the parabolic phase profile is very sensitive to small variations of the effective potential, since $\phi(r,z)$ is directly related to $V(r,z)$. This explains why the prediction (20) is verified for small propagation lengths, $z \lesssim 25L_0$.

D. Correlations in the tail of the incoherent beam

Let us now consider a point beyond the border of the incoherent beam, such that $\nu r^2 \gg 1$ and $\nu^2 r^4/4 - \nu\alpha V_0 z^2 \gg 1$. In this case $R(z) = \sqrt[4]{r_0^4 + 4\alpha V_0 z^2/\nu}$ and

$$\rho(r,\theta,z) = \rho_0(\sqrt[4]{r^4 - 4\alpha V_0 z^2/\nu},\theta)\frac{r^2}{(r^4 - 4\alpha V_0 z^2/\nu)^{1/2}}. \tag{21}$$

This shows that the intensity fluctuations do not exhibit significant variations with respect to the initial condition, $R(z) \simeq r_0 + \alpha V_0 z^2/(\nu r_0^3)$ and $\rho(r,\theta,z) \simeq \rho_0(r,\theta)$.

If we consider a point in the transition region between the two regimes discussed above, i.e., $r = R(z)$ in the tail of the beam such that $\nu r^2 \gg 1$ and $\nu^2 r^4/4 - \nu\alpha V_0 z^2 = O(1)$, we have from Eq. (18), $r_0 = g_\nu^{-1}[\log[R(z)] + \nu^2 R(z)^4/4 - \nu\alpha V_0 z^2]$. If additionally $\nu^2 r^4/4 - \nu\alpha V_0 z^2 < 0$, then $\nu r_0^2 \ll 1$ and $r_0 \simeq R(z)\exp[\nu^2 R(z)^4/4 - \nu\alpha V_0 z^2]$. This corresponds to the situation where the starting point r_0 of the characteristics is inside the support of $V(\boldsymbol{r})$, while the arriving point $r = R(z)$ is outside such a support. Accordingly, $\partial_r V[R(z)] \simeq -2V_0/[\nu R(z)^3]$ and $\partial_r V(r_0) \simeq -2V_0\nu r_0$, which gives

$$\rho(r,\theta,z) = \rho_0\big(re^{\frac{\nu^2 r^4}{4} - \nu\alpha V_0 z^2},\theta\big)\nu^2 r^4 e^{\frac{\nu^2 r^4}{2} - 2\nu\alpha V_0 z^2}. \tag{22}$$

Note that $re^{\frac{\nu^2 r^4}{4} - \nu\alpha V_0 z^2} = O(1)$, but as a function of r it varies very rapidly since we are in the regime $\nu r^2 \gg 1$. This shows that in this region, which is localized around $r \sim \sqrt[4]{4\alpha V_0 z^2/\nu}$,

the speckle pattern varies very rapidly in the radial direction. Notice that this analysis also clarifies the validity domain of Eq. (6). Indeed, the quantum potential term in (3) can be neglected when $\alpha|\nabla^3\rho|/\rho \ll |\nabla V|$. Initially this holds true if $\alpha/\lambda_c^3 \ll \gamma\rho/\sigma$, which is the condition under which the Burgers term $\alpha(\boldsymbol{u}\cdot\nabla)\boldsymbol{u}$ is smaller than ∇V as expressed above through the criterion (7). However as the system evolves the condition becomes stronger. Indeed, when $\alpha\gamma\rho z^2/\sigma^2 \gg 1$, the speckle pattern undergoes strong variations around $r \sim \sqrt[4]{\alpha\gamma\rho z^2\sigma^2}$ as shown by (22). More exactly, the radius of the speckle spots becomes locally of the order of $\lambda_c[\sigma^2/(\alpha\gamma\rho z^2)]$, so that the condition of validity of (6) becomes $[\alpha/\lambda_c^3][(\alpha\gamma\rho z^2)/\sigma^2]^3 \ll \gamma\rho/\sigma$ when $\alpha\gamma\rho z^2/\sigma^2 \gg 1$. When this condition is violated, both the Burgers term and the quantum potential term should be taken into account.

V. CONCLUSION AND PERSPECTIVES

In summary, by considering the NLSE as a representative model, we have shown that highly nonlocal random waves operating in the strongly nonlinear regime are characterized by the spontaneous emergence of long-range phase coherence over a characteristic length scale determined by the amount of nonlocality in the system. We recall that, while the phase of the optical wave exhibits long-range coherence, the beam exhibits pronounced intensity fluctuations. The analysis of the evolution of the intensity fluctuations along the characteristics has revealed that the coherence length can increase in a dramatic way in the radial direction, following the behavior $\sim\exp(\nu\alpha V_0 z^2)$. It is important to emphasize that the formation of long-range phase coherence constitutes a robust phenomenon: Phase coherence emerges almost "instantaneously" for very small propagation lengths, and the simulations reveal that it is preserved in the subsequent evolution even well beyond the singular shock point.

As anticipated, the emergence of long-range phase coherence occurs irrespective of the sign of the nonlinearity. The main difference with respect to the defocusing regime discussed above is that in the focusing case the effective potential is negative $V(r,z) < 0$, so that the orientation of the momentum $\boldsymbol{u}(r,z)$ turns radially *ingoing* toward the center of the beam. Accordingly, the speckles of the incoherent beam get compressed during the propagation, with a corresponding reduction of the coherence length by a factor $\sim\exp(-\nu\alpha|V_0|z^2)$. We finally note that, from a broader perspective, this work provides another remarkable example where critical coherent phase effects strongly impact the dynamical behavior of turbulent optical flows [7,10,11,13,89].

A. Application to multimode optical fibers

The above analysis can be mapped to the problem of linear propagation of a speckle beam in a multimode optical fiber, such as a graded index optical fiber with a potential of the form $V(r) = qr^2$ for $r \leqslant a$, a being the fiber-core radius. By transposing the previous analysis to this problem, phase coherence should emerge in the regime where the effect of the linear potential $V(r)$ dominates diffraction effects, i.e., the regime $\lambda_c \gg \kappa$, where $\kappa = (\alpha/q)^{1/4}$ is the size of the fundamental Gaussian mode. Preliminary numerical simulations confirm the expected emergence of phase coherence for large values of the fiber core, so as to satisfy the requirement that the size of the speckle beam should be much larger than the coherence length, $a > \Delta \gg \lambda_c$. Aside from phase coherence, the simulations evidence a compression of the speckle beam toward the axis of the multimode fiber, in a way similar to the focusing regime discussed here above. Note that such a bunching of ray paths toward the fiber axis may be analyzed by a geometric optics approach (i.e., the regime $\lambda_c \gg \kappa$), although this ray approach is inherently unable to describe the emergence of phase coherence during the propagation of the beam. We also note that the formation of ring-shaped caustics in a waveguide potential has been recently interpreted in relation with the development of dispersive shock waves and the spontaneous formation of autofocusing Airy waves [43]. Although this work deals with the propagation of an initial coherent wave, the analysis may be extended to study the incoherent wave problem considered here.

B. Temporal and spatio-temporal phase coherence

The analysis that we have developed in the spatial case can easily be transposed to the time domain, where one typically studies the temporal dynamics of an incoherent pulse that propagates in a Kerr material featured by a noninstantaneous nonlinear response. The optical field is still governed by a one-dimensional NLSE formally analogous to Eq. (1), in which the transverse spatial variable is mapped to the time variable, and the spatial nonlocal response to the noninstantaneous nonlinear response: $\boldsymbol{r} \to t, U(r) \to R(t), \alpha \to \beta_2/2$ in the NLSE (1), β_2 being the second-order dispersion coefficient of the material. The spatial and temporal versions of the NLSE are then equivalent except that, at variance with the spatial response, the noninstantaneous nonlinear response of the material $[R(t)]$ is constrained by the causality condition [21,90–93]. In complete analogy with the spatial case, temporal phase coherence should emerge in the strongly nonlinear regime in the presence of

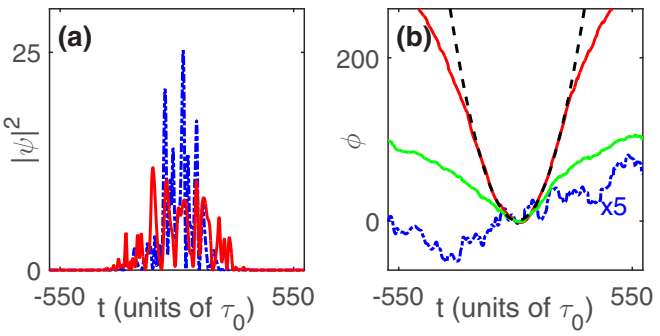

FIG. 6. Emergence of temporal phase coherence: Simulation of the one-dimensional temporal version of the NLSE in the strongly nonlinear regime ($t_c \gg \tau_0$), showing the intensity profile $|\psi|^2(t,z)$ at $z = 0$ (dot-dashed blue line), $z = 80L_0$ (red line) (a), and corresponding unwrapped phases $\phi(t,z)$ at $z = 0$ (dot-dashed blue line), $z = 25L_0$ (green line), $z = 80L_0$ (red line) (b). The dashed-dark line shows a parabolic fit. The initial phase has been multiplied by a factor $\times 5$ for its visibility. Parameters are $\tau_R = 200\tau_0$, size of the temporal numerical window $2048\tau_0$, $\Delta \simeq 120$, $\beta_2\gamma > 0$, $R(t) = H(t)\tau_R^{-1}\exp(-t/\tau_R)$, $H(t)$ being the Heaviside function.

a highly noninstantaneous nonlinear response, $\tau_R \gg t_c \gg \tau_0$, where τ_R is the nonlinear response time, t_c the time correlation, and $\tau_0 = \sqrt{L_0|\beta_2|/2}$ the "healing time." Preliminary simulations realized in this regime confirm that incoherent pulses propagating in slowly responding nonlinear materials are characterized by the emergence of phase coherence over a time scale of the order of the nonlinear response time, as illustrated in Fig. 6. The experimental observation of the spontaneous emergence of temporal phase coherence can be envisaged because of the recent progress made on the fabrication of photonic crystal fibers filled with liquids displaying highly noninstantaneous Kerr responses [92,93].

We finally note that the present analysis in which the emergence of coherence has been studied separately in the spatial or temporal domains, can easily be generalized to the spatio-temporal domain. Recalling the fact that that highly nonlocal nonlinear materials are usually characterized by a slow response time, the emergence of spatio-temporal phase coherence should constitute an important general property of incoherent light propagating in these systems.

ACKNOWLEDGEMENTS

A.P. and A.F. acknowledge support from the Labex ACTION (ANR-11-LABX-01-01) program. A.P. acknowledges funding from the European Research Council under the European Community's Seventh Framework Programme (FP7/20072013 Grant Agreement No. 306633, PETAL project). G.X. acknowledges the support from the ANR project NoAWE (ANR-14-ACHN-0014). C.C. acknowledges funding from the Templeton foundation (Grant No. 58277) and PRIN NEMO (reference 2015KEZNYM). S.T. acknowledges PRIN (2012BFNWZ2). D.F. acknowledges financial support from the European Research Council under the European Unions Seventh Framework Programme (FP/2007-2013)/ERC GA 306559.

[1] R. Z. Sagdeev, D. A. Usikov, and G. M. Zaslavsky, *Nonlinear Physics* (Harwood Publishing, Chur, Switzerland, 1988).
[2] V. E. Zakharov, A. N. Pushkarev, V. F. Shvets, and V. V. Yan'kov, Pis'ma Zh. Eksp. Teor. Fiz. **48**, 79 (1988) [JETP Lett. **48**, 83 (1988)].
[3] B. Rumpf and A. C. Newell, Phys. Rev. Lett. **87**, 054102 (2001).
[4] R. Jordan and C. Josserand, Phys. Rev. E **61**, 1527 (2000).
[5] V. E. Zakharov, F. Dias, and A. Pushkarev, Phys. Rep. **398**, 1 (2004).
[6] J. Laurie, U. Bortolozzo, S. Nazarenko, and S. Residori, Phys. Rep. **514**, 121 (2012).
[7] S. Nazarenko, *Wave Turbulence*, Lecture Notes in Physics (Springer, Berlin, 2011), Vol. 825.
[8] S. Dyachenko, A. C. Newell, A. Pushkarev, and V. E. Zakharov, Physica D **57**, 96 (1992).
[9] A. C. Newell, S. Nazarenko, and L. Biven, Physica D **152-153**, 520 (2001).
[10] C. Connaughton, C. Josserand, A. Picozzi, Y. Pomeau, and S. Rica, Phys. Rev. Lett. **95**, 263901 (2005).
[11] G. Düring, A. Picozzi, and S. Rica, Physica D **238**, 1524 (2009).
[12] P. Aschieri, J. Garnier, C. Michel, V. Doya, and A. Picozzi, Phys. Rev. A **83**, 033838 (2011).
[13] S. Nazarenko, M. Onorato, and D. Proment, Phys. Rev. A **90**, 013624 (2014).
[14] Edited by N. Proukakis, S. Gardiner, M. Davis, and M. Szymańska, Quantum Gases, Finite Temperature and Non-Equilibrium Dynamics, Part II B, *Classical-Field, Stochastic and Field-Theoretic Approaches* (Imperial College Press, London, 2013).
[15] M. J. Davis, S. A. Morgan, and K. Burnett, Phys. Rev. Lett. **87**, 160402 (2001).
[16] N. G. Berloff and B. V. Svistunov, Phys. Rev. A **66**, 013603 (2002).
[17] S. Pitaevskii and L. Stringari, *Bose-Einstein Condensation* (Oxford Science Publications, Oxford, 2003).
[18] J. Klaers, J. Schmitt, F. Vewinger, and M. Weitz, Nature (London) **468**, 545 (2010).
[19] J. Marelic, L. F. Zajiczek, H. J. Hesten, K. H. Leung, E. Y. X. Ong, F. Mintert, and R. A. Nyman, New J. Phys. **18**, 103012 (2016).
[20] A. Chiocchetta, P. E. Larré, and I. Carusotto, Europhys. Lett. **115**, 24002 (2016).
[21] A. Picozzi, J. Garnier, T. Hansson, P. Suret, S. Randoux, G. Millot, and D. Christodoulides, Phys. Rep. **542**, 1 (2014).
[22] C. Conti, M. Leonetti, A. Fratalocchi, L. Angelani, and G. Ruocco, Phys. Rev. Lett. **101**, 143901 (2008).
[23] R. Weill, B. Fischer, and O. Gat, Phys. Rev. Lett. **104**, 173901 (2010).
[24] G. Oren, A. Bekker, and B. Fischer, Optica **1**, 145 (2014).
[25] C. Michel, M. Haelterman, P. Suret, S. Randoux, R. Kaiser, and A. Picozzi, Phys. Rev. A **84**, 033848 (2011).
[26] E. Turitsyna, G. Falkovich, A. El-Taher, X. Shu, P. Harper, and S. Turitsyn, Proc. R. Soc. A **468**, 2496 (2012).
[27] E. Turitsyna, S. Smirnov, S. Sugavanam, N. Tarasov, X. Shu, S. Babin, E. Podivilov, D. Churkin, G. Falkovich, and S. Turitsyn, Nature Photon. **7**, 783 (2013).
[28] I. Carusotto and C. Ciuti, Rev. Modern Phys. **85**, 299 (2013).
[29] M. Vaupel, K. Staliunas, and C. O. Weiss, Phys. Rev. A **54**, 880 (1996).
[30] A. Amo, S. Pigeon, D. Sanvitto, V. G. Sala, R. Hivet, I. Carusotto, F. Pisanello, G. Leménager, R. Houdré, E. Giacobino, C. Ciuti, and A. Bramati, Science **332**, 1167 (2011).
[31] D. Sanvitto, S. Pigeon, A. Amo, D. Ballarini, M. De Giorgi, I. Carusotto, R. Hivet, F. Pisanello, V. G. Sala, P. S. S. Guimaraes, R. Houdré, E. Giacobino, C. Ciuti, A. Bramati, and G. Gigli, Nat. Photonics **5**, 610 (2011).
[32] G. Nardin, G. Grosso, Y. Léger, B. Pietka, F. Morier-Genoud, and B. Deveaud-Plédran, Nature Phys. **7**, 635 (2011).
[33] I. Carusotto, Proc. R. Soc. A **470**, 20140320 (2014).
[34] P.-E. Larré and I. Carusotto, Phys. Rev. A **92**, 043802 (2015).
[35] P.-E. Larré and I. Carusotto, Eur. Phys. J. D **70**, 45 (2016).
[36] D. Vocke, T. Roger, F. Marino, E. M. Wright, I. Carusotto, M. Clerici, and D. Faccio, Optica **2**, 484 (2015).
[37] D. Vocke, K. Wilson, F. Marino, I. Carusotto, E. M. Wright, T. Roger, B. P. Anderson, P. Öhberg, and D. Faccio, Phys. Rev. A **94**, 013849 (2016).
[38] C. Conti, M. Peccianti, and G. Assanto, Phys. Rev. Lett. **92**, 113902 (2004).

[39] N. B. Aleksić, M. S. Petrović, A. I. Strinić, and M. R. Belić, Phys. Rev. A **85**, 033826 (2012).
[40] M. Peccianti and G. Assanto, Phys. Rep. **516**, 147 (2012).
[41] N. Ghofraniha, C. Conti, G. Ruocco, and S. Trillo, Phys. Rev. Lett. **99**, 043903 (2007).
[42] N. Ghofraniha, L. Santamaria Amato, V. Folli, S. Trillo, and E. DelRe, C. Conti. Opt. Lett. **37**, 2325 (2012).
[43] M. Karpov, T. Congy, Y. Sivan, V. Fleurov, N. Pavloff, and S. Bar-Ad, Optica **2**, 1053 (2015).
[44] Z. Chen, S. M. Sears, H. Martin, D. N. Christodoulides, and M. Segev, Proc. Natl. Acad. Sci. U. S. A **99**, 5223 (2002).
[45] C. Rotschild, B. Alfassi, O. Cohen, and M. Segev, Nat. Phys. **2**, 769 (2006).
[46] R. Bekenstein, R. Schley, M. Mutzafi, C. Rotschild, and M. Segev, Nat. Phys. **11**, 872 (2015).
[47] T. Roger, C. Maitland, K. Wilson, N. Westerberg, D. Vocke, E. M. Wright, and D. Faccio, Nat. Commun. **7**, 13492 (2016).
[48] A. Dreischuh, D. N. Neshev, D. E. Petersen, O. Bang, and W. Krolikowski, Phys. Rev. Lett. **96**, 043901 (2006).
[49] Z. Xu, N. F. Smyth, A. A. Minzoni, and Y. S. Kivshar, Opt. Lett. **34**, 1414 (2009).
[50] B. K. Esbensen, A. Wlotzka, M. Bache, O. Bang, and W. Krolikowski, Phys. Rev. A **84**, 053854 (2011).
[51] Q. Kong, M. Shen, Z. Chen, Q. Wang, R.-K. Lee, and W. Krolikowski, Phys. Rev. A **87**, 063832 (2013).
[52] A. Alberucci, C. P. Jisha, and G. Assanto, Opt. Lett. **39**, 4317 (2014).
[53] A. Alberucci, C. P. Jisha, N. F. Smyth, and G. Assanto, Phys. Rev. A **91**, 013841 (2015).
[54] A. Alberucci, C. P. Jisha, and G. Assanto, J. Optics **18**, 125501 (2016).
[55] S. Skupin, O. Bang, D. Edmundson, and W. Krolikowski, Phys. Rev. E **73**, 066603 (2006).
[56] F. Maucher, T. Pohl, S. Skupin, and W. Krolikowski, Phys. Rev. Lett. **116**, 163902 (2016).
[57] W. Krolikowski, O. Bang, N. I. Nikolov, D. Neshev, J. Wyller, J. J. Rasmussen, and D. Edmundson, J. Opt. B: Quant. Semicl. Opt. **6**, S288 (2004).
[58] S. Bar-Ad, R. Schilling, and V. Fleurov, Phys. Rev. A **87**, 013802 (2013).
[59] L. Zhong, Y. Li, Y. Chen, W. Hong, W. Hu, and Q. Guo, Sci. Rep. **7**, 41438 (2017).
[60] M. A. Baranov, Phys. Rep. **464**, 71 (2008).
[61] C. Josserand, Y. Pomeau, and S. Rica, Phys. Rev. Lett **98**, 195301 (2007).
[62] S. Skupin, M. Saffman, and W. Krolikowski, Phys. Rev. Lett. **98**, 263902 (2007).
[63] S. Sevincli, N. Henkel, C. Ates, and T. Pohl, Phys. Rev. Lett. **107**, 153001 (2011).
[64] V. E. Zakharov, S. L. Musher, and A. M. Rubenchik, Phys. Rep. **129**, 285 (1985).
[65] A. Minovich, D. N. Neshev, A. Dreischuh, W. Krolikowski, and Y. S. Kivshar, Opt. Lett. **32**, 1599 (2007).
[66] P. R. Holland, *The Quantum Theory of Motion* (Cambridge University Press, Cambridge, 1993).
[67] A. Picozzi and J. Garnier, Phys. Rev. Lett. **107**, 233901 (2011).
[68] G. Xu, D. Vocke, D. Faccio, J. Garnier, T. Roger, S. Trillo, and A. Picozzi, Nature Comm. **6**, 8131 (2015).
[69] G. Xu, J. Garnier, D. Faccio, S. Trillo, and A. Picozzi, Physica D **333**, 310 (2016).
[70] A. Campa, T. Dauxois, D. Fanelli, and S. Ruffo, *Physics of Long-Range Interacting Systems* (Oxford University Press, Oxford, 2014).
[71] G. B. Whitham, *Linear and Nonlinear Waves* (Wiley, New York, 1974).
[72] W. Wan, S. Jia, and J. W. Fleischer, Nat. Phys. **3**, 46 (2007).
[73] J. Fatome, C. Finot, G. Millot, A. Armaroli, and S. Trillo, Phys. Rev. X **4**, 021022 (2014).
[74] M. A. Hoefer, M. J. Ablowitz, I. Coddington, E. A. Cornell, P. Engels, and V. Schweikhard, Phys. Rev. A **74**, 023623 (2006).
[75] J. A. Joseph, J. E. Thomas, M. Kulkarni, and A. G. Abanov, Phys. Rev. Lett. **106**, 150401 (2011).
[76] P. Whalen, J. V. Moloney, A. C. Newell, K. Newell, and M. Kolesik, Phys. Rev. A **86**, 033806 (2012).
[77] B. Wetzel, D. Bongiovanni, M. Kues, Y. Hu, Z. Chen, S. Trillo, J. M. Dudley, S. Wabnitz, and R. Morandotti, Phys. Rev. Lett. **117**, 073902 (2016).
[78] S. Trillo, G. Deng, G. Biondini, M. Klein, G. F. Clauss, A. Chabchoub, and M. Onorato, Phys. Rev. Lett. **117**, 144102 (2016).
[79] M. Onorato, S. Residori, and F. Baronio (Eds.), *Rogue and Shock Waves in Nonlinear Dispersive Media*, Lecture Notes in Physics (Springer, Berlin, 2016), Vol. 926.
[80] G. A. El and N. F. Smyth, Proc. R. Soc. A **472**, 20150633 (2016).
[81] S. Gentilini, M. C. Braidotti, G. Marcucci, E. DelRe, and C. Conti, Phys. Rev. A **92**, 023801 (2015).
[82] S. A. Akhmanov, D. P. Krindach, A. P. Sukhorukov, and R. V. Khokhlov, ZhETF Pis'ma **6**, 509 (1967) [JETP Lett. **6**, 38 (1967)].
[83] S. A. Akhmanov, D. P. Krindach, A. V. Migulin, A. P. Sukhorukov, and R. V. Khokhlov, IEEE J. Quantum Electron. **4**, 568 (1968).
[84] J. R. Whinnery, D. T. Miller, and F. Dabby, IEEE J. Quantum Electron. **3**, 382 (1967).
[85] G. P. Gordon, R. C. C. Leite, R. S. Moore, S. P. S. Porto, and J. R. Whinnery, J. Appl. Phys. **36**, 3 (1965).
[86] N. Ghofraniha, S. Gentilini, V. Folli, E. DelRe, and C. Conti, Phys. Rev. Lett. **109**, 243902 (2012).
[87] A. Fratalocchi, A. Armaroli, and S. Trillo, Phys. Rev. A **83**, 053846 (2011).
[88] J. Garnier, G. Xu, S. Trillo, and A. Picozzi, Phys. Rev. Lett. **111**, 113902 (2013).
[89] M. Guasoni, J. Garnier, B. Rumpf, D. Sugny, J. Fatome, F. Amrani, G. Millot, and A. Picozzi, Phys. Rev. X **7**, 011025 (2017).
[90] C. Michel, B. Kibler, J. Garnier, and A. Picozzi, Phys. Rev. A **86**, 041801(R) (2012).
[91] G. Xu, J. Garnier, and A. Picozzi, Opt. Lett. **39**, 590 (2014).
[92] C. Conti, M. A. Schmidt, P. S. J. Russell, and F. Biancalana, Phys. Rev. Lett. **105**, 263902 (2010).
[93] M. Vieweg, T. Gissibl, S. Pricking, B. T. Kuhlmey, D. C. Wu, B. J. Eggleton, and H. Giessen, Opt. Express **18**, 25232 (2010).